Available online at www.easdprocedia.org
EASD Procedia EURODYN (2020) 1358-1372

EASD Procedia

EURODYN 2020
XI International Conference on Structural Dynamics
M. Papadrakakis, M. Fragiadakis, C. Papadimitriou (eds.)
Athens, Greece, 23–26 November 2020

COMPARISON OF ALTERNATIVE DYNAMIC VIBRATION MITIGATION APPROACHES FOR WIND TURBINE TOWERS

K. A. Kapasakalis[1], P.O.N. Bollano[1], E. J. Sapountzakis[1], and I. A. Antoniadis[2]

[1] Institute of Structural Analysis and Antiseismic Research, School of Civil Engineering, National Technical University of Athens,
Zografou Campus, GR-157 80 Athens, Greece
kostiskapasakalis@hotmail.com, orfeabollano@hotmail.com, cvsapoun@central.ntua.gr

[2] Dynamics and Structures Laboratory, School of Mechanical Engineering, National Technical University of Athens,
Zografou Campus, GR-157 80 Athens, Greece
antogian@central.ntua.gr

Keywords: Wind turbines; Negative stiffness; Vibration absorption; KDamper; damping;

Abstract. *The application of vibration absorbers to Wind Turbine (WT) towers has the potential to significantly improve the damping of the tower and the nacelle dynamic response, increasing thus the reliability of WTs. The Tuned Mass Damper (TMD) is considered as a benchmark design option for vibration absorption in Wind Turbine towers. However, its effectiveness is limited by the requirement of large masses, in association with its installation location (top of the WT tower). For this reason, two alternative concepts are considered. First, the nacelle is released from the Wind Turbine tower (nacelle isolation concept), using a low stiffness connection. This option is based on the seismic isolation concept of structures with the use of seismic isolation bearings. Alternatively, a novel passive vibration absorption concept is implemented, based on the KDamper concept. The KDamper is essentially based on the TMD, including however an additional negative stiffness element. Instead of increasing the additional mass, the vibration absorption capability of the KDamper can be increased by increasing the value of the negative stiffness element. Thus, the KDamper always indicates better isolation properties than a TMD damper with the same additional mass. In this paper, the performance of these three vibration absorption concepts is examined for increasing the damping of Wind Turbine towers and for the improvement of their dynamic response. Although all methods present a good behavior, the proposed vibration absorption systems present a significant increase of the damping ratio with a minimal value of added mass at the top of the tower.*

ISSN:2311-9020
Peer-review under responsibility of the Organizing Committee of EURODYN 2020.
doi: 10.47964/1120.9110.20133

1 INTRODUCTION

As wind power continues its rapid growth worldwide, wind farms have a high probability to comprise a significant portion of the total production of wind energy, and can even become a hefty contributor to the total electricity production in some countries. The high-quality wind resource and the closeness to load centers make wind energy a fascinating proposition. The Wind Turbine (WT) is supported by a tower that can experience extreme vibrations caused by both the wind turbine and the wind forces due to its geometry and great height. An accurate analysis of the structural behavior of the tower is of high importance due to its cost, which can represent roughly 20% of the total cost of the system [1]. A lot of researchers have been studying the use of structural control to help overcome the wind-induced vibrations experienced by Wind Turbine towers[2]–[5]. The passive control methods are plain and trustworthy. They do not require an external force, are easy to implement to reduce the structural vibration and are widely used in Wind Turbine technology for the improvement of their damping. They incorporate one or more devices to the main structure to absorb or transfer part of its energy.

The intention with the installation of such devices, for the control of Wind Turbine towers, is the mitigation of their dynamic response because of the fact that the vibrations caused by aerodynamic loads are longstanding and cause fatigue problems to the body of the tower and their foundation.

The installation of a resonant damper like a Tuned Mass Damper (TMD) is the damping concept that has obtained the most consideration in the literature. A Tuned Mass Damper (TMD) is a control device that consists of a mass-spring-dashpot attached to the structure, intending to reduce structural vibration response [6], [7]. The TMD concept was first applied by (Frahm, 1909 [8]). A theory for the TMD was introduced in the paper by (Ormondroyd and Den Hartog, 1928 [9]). A detailed discussion of optimal tuning and damping parameters appears in (Den Hartog, 1956 [10]). Since then, a great number of applications of various forms of TMDs have been reported. Some new examples include vibration absorption in seismic or other forms of excitation of structures (Debnath et al., 2015 [11]). TMDs are available in various physical forms, including solids, liquids, or active implementations (Younespour and Ghaffarzadeh, 2015 [12]). The Active Tuned Mass Damper (ATMD) is a hybrid device comprising of a passive TMD supplemented by an actuator parallel to the spring and damper. It is a well-known concept in structural control and has demonstrated enhanced damping performance compared to the passive TMD [13], [14]. The drawback of such designs is that their performance is directly dependent on the accuracy of the actuator's output, which over time can have alterations in its performance by false estimation of the desired function of the vibration absorption concept. Various forms of Dynamic Vibration Absorbers (DVA) have been used, such as Tuned Liquid Column Damper (TCLD) or a Tuned Mass Damper (TMD). Some of the pioneering work regarding applications in wind turbines include the work by Colwell and Basu [15] in which the damping effect of a TLCD installed in an offshore wind turbine has been examined by assuming correlated wind and wave load conditions. A different geometry of the TMD is the pendulum device [16]. The main structure excites the device, and part of its energy is transferred by its movement and then it is dissipated by the pendulum damper.

In order to be potent, a resonant damper like a TMD should be installed where the absolute motion of the targeted vibration mode is largest, which is at the top of the tower or inside the nacelle. Effective damping by a TMD is correlated with a large damper mass, which forms a major limitation since additional mass is undesirable at the top of the wind turbine.

For this reason, two alternative vibration mitigation concepts are examined in this paper. First, the nacelle is released from the Wind Turbine tower (nacelle isolation concept), using a low stiffness connection. This is the most well-known path to earthquake-resistance designs as

it is based on the concept of reducing the seismic demand instead of increasing the structure's resistant capacity. Modern seismic isolation systems for structures grant horizontal isolation from the seismic effects, by decoupling the structure from its foundation [17]–[21]. Among others, this concept has been shown to behave effectively in bridge decks, supported on flexible piers [22], [23].

Alternatively, the KDamper concept, proposed in Antoniadis et al. 2016 [24], is studied. The KDamper extends the classical Tuned Mass Damper by integrating appropriate negative stiffness elements, rather than increasing the additional mass, which enhances the capability of the KDamper, overcoming the sensitivity problems of TMDs as the tuning is primarily controlled by the negative stiffness element's parameters. Although the KDamper incorporates a negative stiffness element, it is drafted to be both statically and dynamically stable. The KDamper is examined for the protection of bridge structures [25]–[29], Wind Turbines [30], [31] and structural systems [32], [33]. In addition, the KDamper is implemented as an Absorption Base (KDAB) in the bases of structures [34]–[40].

Section 2 of the paper demonstrates the methodology and the modeling procedure for the three approaches. Section 3 presents the method of the optimal selection of the parameters of the three approaches. Section 4 presents a comparison of the approaches with respect to the improvement of the dynamic performance of the Wind Turbine Tower and of the nacelle.

2 METHODOLOGY AND MODELING

The contemporary design of wind turbines requires power rates of more than 5MW which can be accomplished by wider rotors (diameters of more than 120 m); for that reason, a proportionate increase of the tower height is required. However, this height increase has immediate effects on the structural behavior of the wind turbine because of the augmented wind pressure area and the slenderness of the tower. Moreover, considering that both the tower and the foundation are vital components of the wind turbine, reaching a rather large percentage of the overall turbine budget (over 60% including the installation cost) [41], [42] the improvement of the dynamic response of the wind turbine tower is of high importance. In this work, a steel tower of 120 m height that supports the NREL baseline 5-MW nacelle and rotor, is used. The key properties of the wind turbine and the steel tower are listed in Table 1 and Table 2 respectively.

Property	**Value**
Rating	5 MW
Rotor diameter	126 m
Hub diameter	3 m
Cut-in wind speed	3 m/sec
Rated wind speed	11.4 m/sec
Cut-out wind speed	25 m/sec
Cut-in rotor speed	6.9 rpm
Rated rotor speed	12.1 rpm
Nacelle mass	240,000 kg
Rotor mass	110,000 kg
Blade material	Glass-fibre
Blade length	61.5 m
Blade mass	17,740 kg
Blade CM (from blade root)	20.475 m
Blade damping ratio (all modes)	0.48%

Table 1: Key properties of NREL baseline 5 MW wind turbine.

Property	Value
Height	120 m
Base diameter	8.43 m
Base steel thickness	0.048 m
Top diameter	3.87 m
Top steel thickness	0.025 m
Young's modulus	210 GPa
Steel density	8,500 kg/m^3
Total mass	798,640 kg
Location of CM (above base)	43.042 m
Tower damping ratio (all modes)	2%

Table 2: Key properties of the considered steel tower.

2.1 Vibration mitigation concepts considered

Fig. 1 displays the dynamic vibration absorber design options that will be analyzed in this paper. The first vibration absorption concept is based on the classical tuned mass damper (TMD). Figure 1i presents the schematic image of the TMD concept. An additional mass is attached to the top of the wind turbine tower or inside the nacelle, using a positive stiffness element and a linear damper. The main disadvantage is the need for a large additional mass in order for TMD to attain effective damping. Figure 1ii presents the nacelle-isolation vibration absorption concept, where the mass that correlates to the mechanical parts (nacelle, rotor, and blades) is used as an additional mass of a TMD. The additional mass is no more connected rigidly to the steel tower but is accomplished with a stiffness connection and a linear damper, as in the case of the classical TMD concepts. Figure 1iii presents the realization of the KDamper concept [24] in a wind turbine tower. Again, as in the nacelle-isolation concept, the additional mass of the nacelle, rotor, and blades is no longer rigidly attached to the wind turbine tower but through the interference of a KDamper device. This time the additional mass of the vibration absorption concept is connected with the mass that corresponds to the nacelle, rotor, and blades with a positive stiffness element and a linear damper, and with the top of the wind turbine tower with a negative stiffness element.

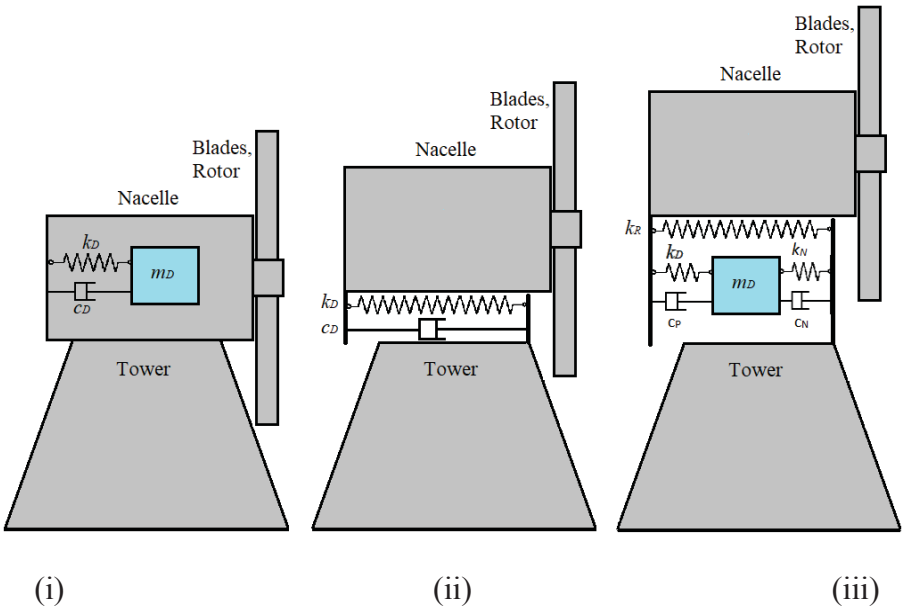

Fig. 1: Schematic representation of the considered vibration absorption concepts, (i) TMD concept, (ii) Nacelle-isolation concept and (iii) KDamper concept.

2.2 Dynamic model of the wind turbine

A wind turbine tower (Table 2) of variable tubular cross-section supporting the NREL baseline 5-MW nacelle and rotor [42] is examined. In order to consider the inertial forces applied by the mechanical parts (nacelle, rotor, and blades), an additional mass concentrated at the top, *mtop*=403.22 tn [42] is added at the top of the tower.

The equations of motion of the wind turbine including the respective vibration mitigation concept to be considered are obtained by analyzing the equilibrium of forces at the location of each degree of freedom as follows:

$$[M_S]\{\ddot{x}_S\}+[C_S]\{\dot{x}_S\}+[K_S]\{x_S\}=[P] \tag{1}$$

Where $[M_S]$, $[C_S]$ and $[K_S]$ are the mass, damping and stiffness matrices of the controlled wind turbine tower, respectively of order $(N+n)$ *x* $(N+n)$. Here, N suggests the degrees of freedom (DoF) for the wind turbine tower and n indicates the DoF of each of the vibration isolation options to be considered. In this paper, the degrees of freedom for the wind turbine tower is N=24. The mass matrix is of order $(N+n)$ *x* $(N+n)$ as follows:

$$[M_S]=\left[\begin{bmatrix}[M_N]_{N\times N} & [0]_{N\times n}\\ [0]_{n\times N} & [0]_{n\times n}\end{bmatrix}+\begin{bmatrix}[M_{n,a}]_{N\times N} & [0]_{N\times n}\\ [0]_{n\times N} & [M_{n,d}]_{n\times n}\end{bmatrix}\right]_{(N+n)\times(N+n)} \tag{2}$$

Where $[M_N]_{NxN}$ is the mass matrix of the uncontrolled wind turbine tower and $[M_n]_{nxn}$ indicates the mass matrix of the vibration isolation concept. The condensed stiffness matrix $[K_N]_{NxN}$ of the uncontrolled wind turbine tower is correlating to the sway degrees of freedom taken as the dynamic DoF. The damping matrix $[C_N]_{NxN}$ is not precisely known but is obtained with the help of the Rayleigh's approach using the same damping ratio in all modes, 2%. The stiffness matrix $[K_N]_{NxN}$ and the damping matrix $[C_N]_{NxN}$ are expressed in agreement to the degrees of freedom associated with the respective vibration isolation system to be considered.

The stiffness and damping matrix of the controlled system are formed as follows:

$$[K_S]=\left|\begin{bmatrix}[K_N]_{N\times N} & [0]_{N\times n}\\ [0]_{n\times N} & [0]_{n\times n}\end{bmatrix}+\begin{bmatrix}[K_{n,a}]_{N\times N} & -[K_{n,b}]_{N\times n}\\ -[K_{n,c}]_{n\times N} & [K_{n,d}]_{n\times n}\end{bmatrix}\right|_{(N+n)\times(N+n)} \tag{3}$$

$$[C_S]=\left|\begin{bmatrix}[C_N]_{N\times N} & [0]_{N\times n}\\ [0]_{n\times N} & [0]_{n\times n}\end{bmatrix}+\begin{bmatrix}[C_{n,a}]_{N\times N} & -[C_{n,b}]_{N\times n}\\ -[C_{n,c}]_{n\times N} & [C_{n,d}]_{n\times n}\end{bmatrix}\right|_{(N+n)\times(N+n)} \tag{4}$$

The coupled differential equations of motion (Eq.11111) for t1111he isolated wind turbine tower are thus derived and solved using Newmark's integration method.

The wind turbine tower is modeled as a Generalized Single Degree of Freedom System with a shape function based on the first modal eigenform of the non-isolated wind turbine tower. The additional concentrated mass of 403.22 tn, is placed together with the tower's mass m_B. Therefore, the system's parameters are: m_B = 80.57 tn, k_B = 1977.47 kN/m, c_B = 8kN*s/m. Additional assumptions made for the detailed formulation are: (i) the wind turbine tower is considered to remain within the elastic limit under the aerodynamic loads; and (ii) the effects of soil-structure-interaction (SSI) are not taken into account.

2.3 Aerodynamic load

The loading due to the wind is taken into consideration as follows. The tower is deemed to be subjected to the horizontal force $\overline{F}_N(t)$ due to the wind at its top. Moreover, the horizontal force $F_{Nr}(r, t)$ acting as a position r along the wind turbine blade can be acquired by the following relation [43]:

$$F_{N_r}(\mathrm{r},\mathrm{t}) = \frac{1}{2}\rho_{air} C_N(r) c_{bl}(r)(\overline{V}(t))^2 \tag{5}$$

Where ρ_{air} = 1.225 x 10^{-3} tn/m^3 is the air density and $C_N(r)$ is the coefficient calculated by the corresponding lift $C_L(r)$ and drag $C_D(r)$ coefficients. The values of the latter coefficients depend on the airfoil characteristics of the blades and their distribution with consideration to the "angle of attack" of the wind velocity $\overline{V}(t)$ vector passing through the blade profile can be retrieved from. It is noted that $\overline{V}(t)$ is presumed to have a uniform spatial distribution over the actuator disc. $c_{bl}(r)$, $\beta(r)$ is the chord and the pitch angle of the blade profile fluctuating along the blade length r, the distributions of which are acquired according to the blade type employed to equip the turbine. $C_N(r)$ is given as:

$$C_N(\mathrm{r}) = C_L(r)\cos\varphi(\mathrm{r}) + C_D(r)\sin\varphi(r) \tag{6}$$

Where $\varphi(r)$ is the wind flow angle [43]. In order to calculate $\varphi(r)$ and consequently $C_N(r)$, the blade element momentum theory incorporating Prandtl's tip loss factor and Glauert's correction [43] is utilized with a hypothesis of constant angular velocity of the blades $\boldsymbol{\Omega_{bl}}$. Subsequently, breaking $\overline{V}(t)$ down into a mean component V_m and a fluctuating component $V(t)$, the corresponding mean and fluctuating components of $F_{Nr}(r, t)$ can be obtained as:

$$F_{Nm} = \frac{1}{2}\rho_{air} C_N(r) c_{bl}(r) V_m^2 \tag{7}$$

$$F_N(r,t) = \frac{1}{2}\rho_{air} C_N(r) c_{bl}(r)(2V_m V(t) + V(t)^2) \tag{8}$$

In this work, the mean velocity is gained by using a basic velocity at an altitude of 10 m, V_b and applying the corresponding regulations of EC1, Part1,4 [44]. Moreover, in order to take into consideration the wind velocity fluctuation at the altitude of l_t, an artificial velocity time history is produced applying the procedures presented in References [45]–[47]assuming a value of standard deviation σ. After having established $F_{Nr}(r,t)$, the total concentrated force exerted on the top of the tower can be computed as:

$$\overline{F}_N(t) = 3\int_0^{r_{bl}} \overline{F}_N(r,t)dr \tag{9}$$

Besides the concentrated force applied on the top of the tower because of the operation of the turbine, the distributed loading along the tower height is not taken into account due to the fact that it has a minimal influence on the dynamic response of the tower. The basic wind velocity that is employed has equivalent standard deviations V_b = 27.0 m/s with σ = 3.30 m/s ($V_\mathrm{m}(120)$ = 39.93 m/s). The rotor is presumed to develop a constant angular velocity $\boldsymbol{\Omega_{bl}}$ = 12.1 rpm, while all the necessary blade profile characteristics are retrieved from References [42] and [48] (Fig. 2(i)).

Also, a different type of load (Fig. 2(ii)) is employed for the simulation as described in Shkara et al. [49] so that a proper time history of the aerodynamic loads induced to the tower is

obtained, that accurately depicts the alterations of the aerodynamic load in relation with the motion of the wind turbine blades. The basic wind velocity that is aforementioned is still employed in accordance with the response described in [49]. The figure represents the time history of the load for ten seconds but the simulation is performed for a hundred seconds.

The total force $\overline{F}_N(t)$ applied at the top of the wind turbine tower is an instantaneously imposed load that is slowly changing over time. Therefore, for each case separately, in order to properly calculate the maximum permanent displacement of the oscillation of the tower, the first value of the total force $\overline{F}_N(t)$ is deducted from all the values of the total force so that the fatigue simulation is conducted without the instantaneous imposing of the load interfering with the response of the tower.

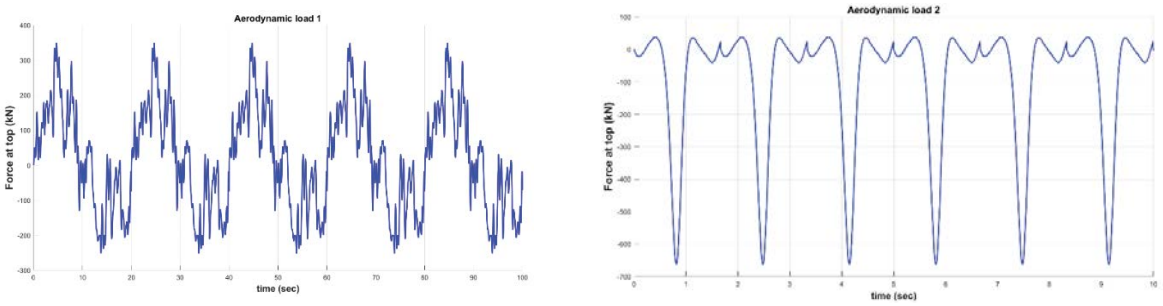

(i) (ii)

Fig. 2: The two different types of loads: (i) Aerodynamic load based on EC1[44], (ii) Aerodynamic load based on Shkara et al. [49].

3 OPTIMIZATION OF THE VIBRATION MITIGATION CONCEPTS

3.1 Harmony search algorithm and optimization process

In this section, the HS metaheuristic algorithm is shortly described and is also presented with a comprehensive example of the recommended optimization procedure. The four key steps of the algorithm are presented below:

Step 1: Initialization of the HS Memory matrix (HM). HM matrix consists of vectors representing potential solutions to the examined optimization problem. The original HM matrix is formed using randomly generated results. For an n-dimension problem, HM has the form:

$$HM = \begin{bmatrix} x_1^1, x_2^1, \ldots, x_n^1 \\ x_1^2, x_2^2, \ldots, x_n^2 \\ \cdot \\ \cdot \\ \cdot \\ x_1^{HMS}, x_2^{HMS}, \ldots, x_n^{HMS} \end{bmatrix} \tag{10}$$

where $[x^1_1, x^1_2, \ldots, x^1_n]$ ($i=1, 2, \ldots, HMS$) is a result candidate. HMS is generally set to values between 50 and 100. The value of the objective function is determined for every solution vector of the HM matrix.

Step 2: Improvisation of a $[x'_1, x'_1, \ldots, x'_1]$ new result from the HM. Each one of the components of this new result, x'_j, is gained based on the Harmony Memory Considering Rate (HMCR), which is described as the probability of selecting a component from the HM members. 1 – HMCR is, thus, the probability of creating a new component at random. If x'_j is elected from

the HM matrix, it is further altered according to the Pitching Adjusting Rate (PAR), which regulates the probability of a candidate from the HM to be altered.

Step 3: Update of the HM matrix. The value of the objective function of the new result, gained in Step 2, is determined and measured to the ones that correlate to the original HM matrix vectors. If the outcome is a better fitness than that of the worst member in the HM, it will take over that one. If there is more than one member in the HM with bigger values of the objective function that the new solution, the result with the higher value is replaced. Otherwise, the new solution is erased and the HM matrix remains untouched.

Step 4: Repetition of Steps 2 and 3 until a preset termination benchmark is satisfied. A frequently used termination benchmark is the maximum number of total iterations.

The flowchart of the suggested HS algorithm is shown in Fig. 3.

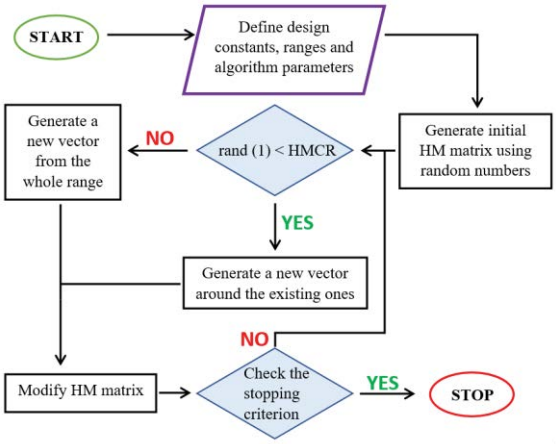

Fig. 3: Flowchart of the proposed HS algorithm.

3.2 Vibration mitigation concepts optimization process

Succeeding the method and flowchart presented above, the features of the inspected optimization problems can be calculated.

First of all, the parameters are selected, whose values shall be optimized for each concept. The KDamper concept has five parameters that control the device's performance and those are k_R, k_D, k_N, c_N, c_p. The additional mass ratio of the KDamper device is selected equal to 1%. The TMD concept has a single parameter ζ_D since the mass ratio is selected equal to 5% and k_D is selected so that the natural period T of the TMD is equal to that of the tower modeled as a Generalized SDOF. The TMD-Nacelle concept has two parameters that control the device's performance, k_D and ζ_D. Furthermore, the restrains of the design variables are decided. Their choice relies on safety, stability and manufacturing parameters that need to be considered. Although these parameters may alter from structure to structure, the restraints presented below produce satisfying results in most cases.

	k_R	k_D(KDamper)	k_N	c_N	c_p	ζ_D(TMD)	k_D(TMD-Nacelle)	ζ_D(TMD-Nacelle)
min	0	0	-40000	0	0	0	0	0
max	120000	120000	0	500	500	1	20000	0.5

Table 3: Variable design limits.

As far as the parameters inherently involved in the HS algorithm are concerned, a common practice is to adopt commonly found values found in relative literature (Table 4). The same is true for the termination criterion, as the maximum number of repetitions is pre-determined.

HMS	HMCR	PAR
75	0.5	0.1

Table 4: Values of the HS algorithm parameters

With the intention of finding the optimum solution for the EC1 [44] aerodynamic load, the top of the tower's displacement is determined as the objective function that needs to be minimized, in each case.

Finally, the constraints and limitations of the inspected optimization problem are specified. Specifically, for the KDamper concept, there are three constraints, the first one demanding that the relative displacement of the additional mass of the KDamper be lower than 1.5 *m*, the second one demanding that the absolute velocity of the nacelle must be lower than 1 *m/sec* and the third one demanding that the relative displacement of the nacelle to the top of the tower be lower than 0.5 *m*. The last two constraints also apply to the other two concepts.

4 COMPARISON OF THE PROPOSED CONCEPTS

The design criterion of the Tuned Mass Damper and KDamper vibration absorption concepts is their mass ratio, which corresponds to the additional mass added to the system, and for the nacelle-isolation concept is that the maximum relative displacement, between the nacelle and the tower, must be under 0.5 m. The mass ratio of the TMD is selected 5% (as a maximum value for constructional reasons), the mass ratio of the KDamper 1% and the relative displacement between the nacelle and the tower, for the nacelle-isolation concept is 0.5 *m*. The exact values derived from the optimization process for each of the employed vibration absorption concepts are the following: (i) KDamper: k_R = 7296 *kN/m*, k_D = 114272 *kN/m*, k_N = -6234 *kN/m*, c_N = 345 *kNs/m*, c_p = 300 *kNs/m*, (ii) TMD: ζ_D = 0.04, (iii) TMD-Nacelle: k_D = 606 *kN/m*, ζ_D= 0.32.

In Table 5 and Table 6, are the results (maximum values) of the controlled wind turbine concerning the dynamic performance of the wind turbine tower for both load cases. In Table 7 are the results (mean values) of the energy dissipated by the dampers of each of the proposed concepts.

	$U_{abs,\,top}$ (m)	$V_{abs,nacelle}$ (m/s)
Initial	0.5851	1.0455
KDamper	0.1607	0.4836
TMD	0.3111	0.5275
TMD-Nacelle	0.1601	0.4920

Table 5: Maximum values of the controlled wind turbine's tower dynamic performance for Aerodynamic load 1.

	$U_{abs,\,top}$ (m)	$V_{abs,nacelle}$ (m/s)
Initial	0.1477	0.2964
KDamper	0.0925	0.3185
TMD	0.1442	0.2825
TMD-Nacelle	0.0960	0.3267

Table 6: Maximum values of the controlled wind turbine's tower dynamic performance for Aerodynamic load 2.

W_d (kW)	Aerodynamic load 1	Aerodynamic load 2
KDamper	8.5373	0.9049
TMD	5.4562	0.1242
TMD-Nacelle	15.6352	2.9603

Table 7: Mean value of the energy dissipated per cycle by the proposed vibration absorption concepts for each aerodynamic load.

In the following figures Fig. 4,Fig. 5,Fig. 6,Fig. 7) are depicted the time-histories of the tower top displacement and the nacelle's velocity for both the aerodynamic loads and for all the vibration absorption concepts so that a more immediate and clear comparison can be made between the proposed concepts. Also in Fig. 8 and Fig. 9 the dissipated energy through the oscillation duration is depicted so that a clear picture can be obtained on whether this energy can be exploited.

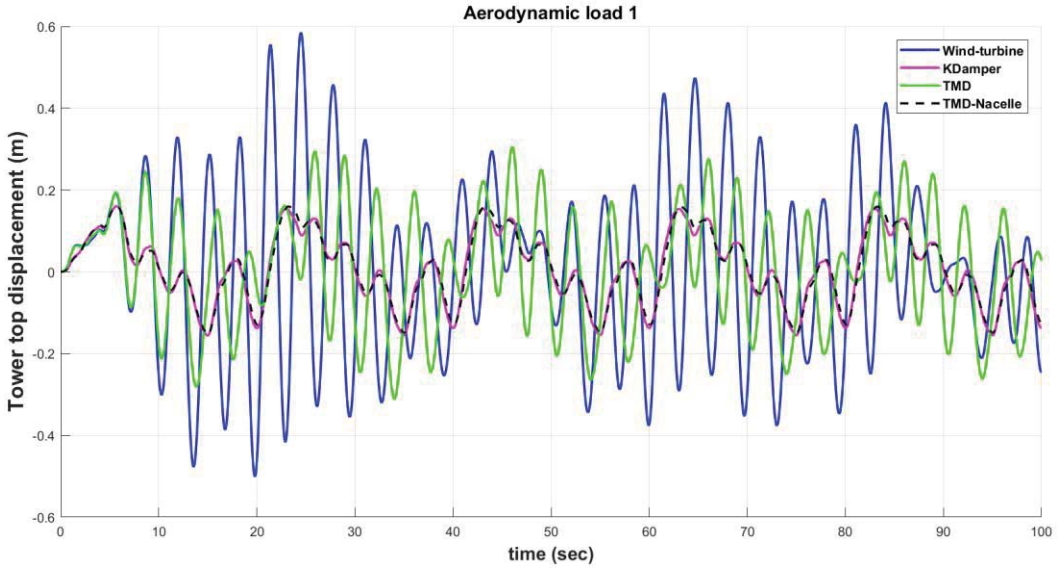

Fig. 4: Time history of tower top displacement for aerodynamic load 1

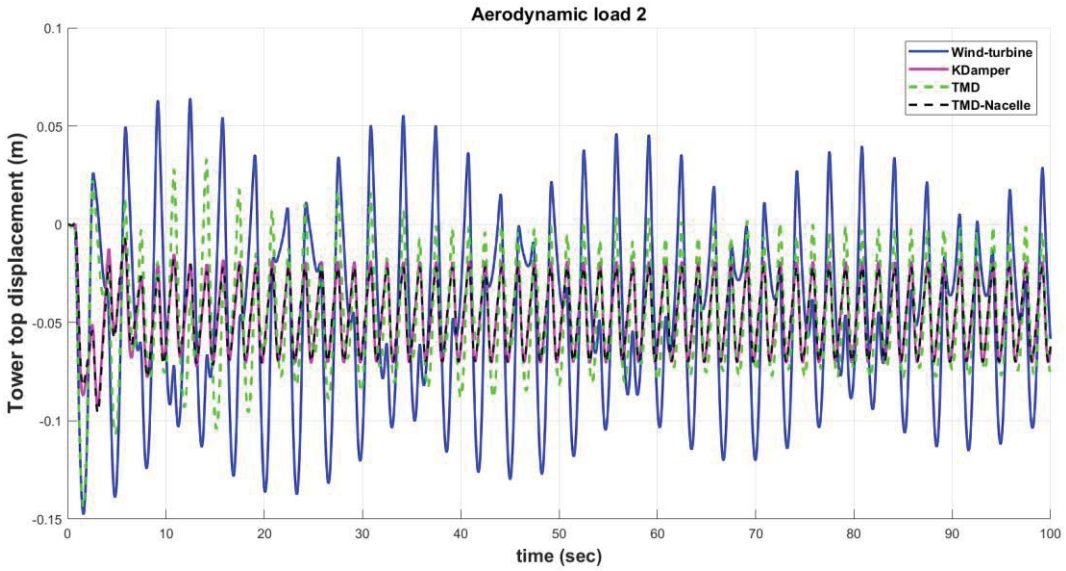

Fig. 5: Time history of tower top displacement for aerodynamic load 2

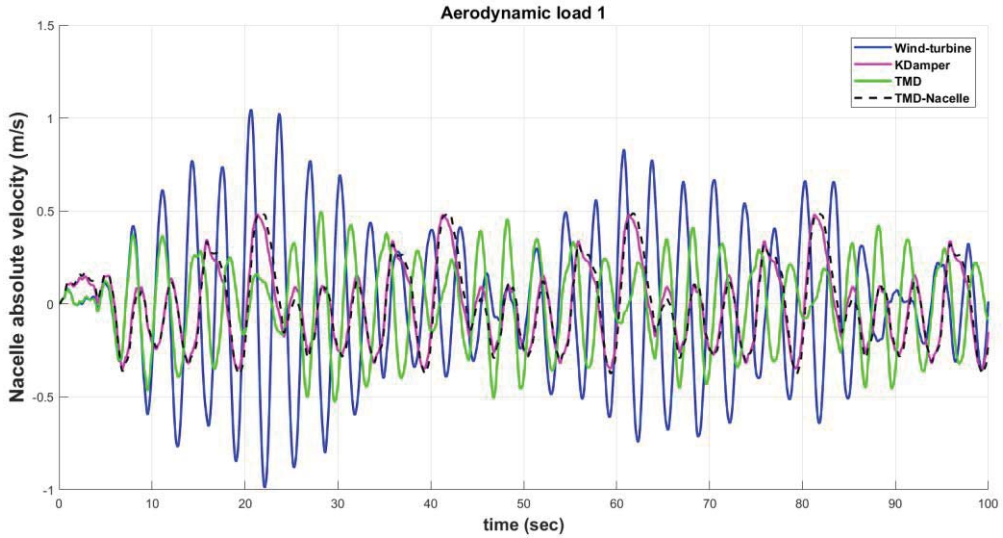

Fig. 6: Time history of nacelle's absolute velocity for aerodynamic load 1

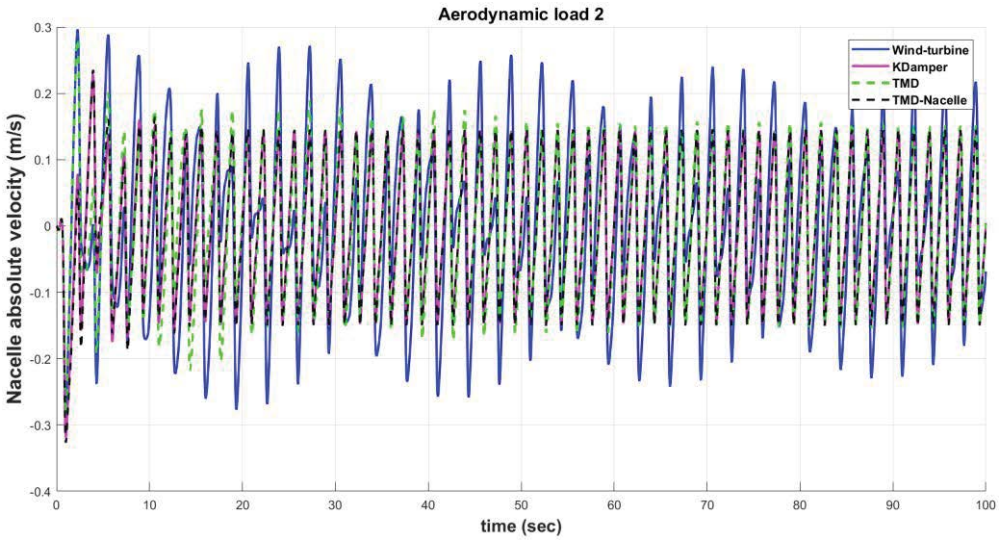

Fig. 7: Time history of nacelle's absolute velocity for aerodynamic load 2

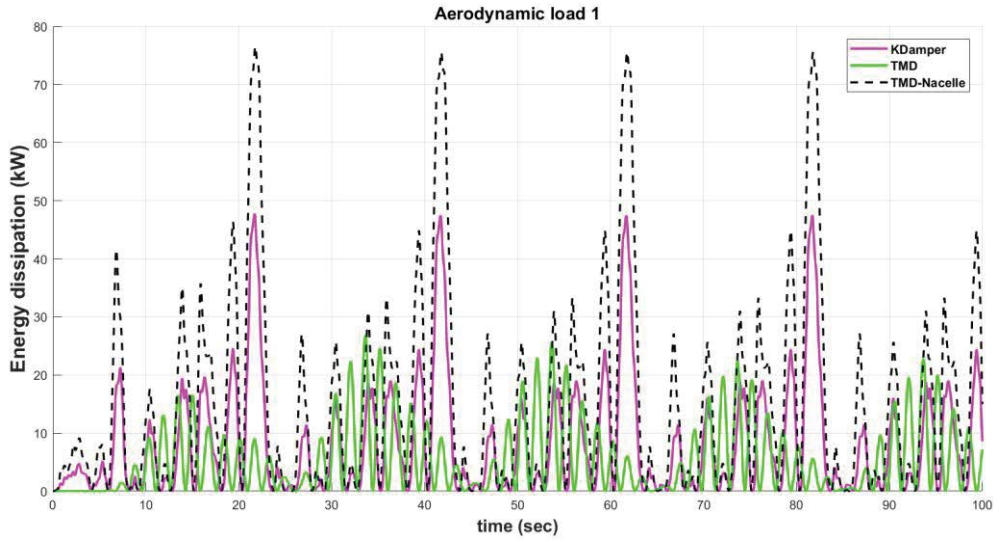

Fig. 8: Energy dissipation for Aerodynamic load 1

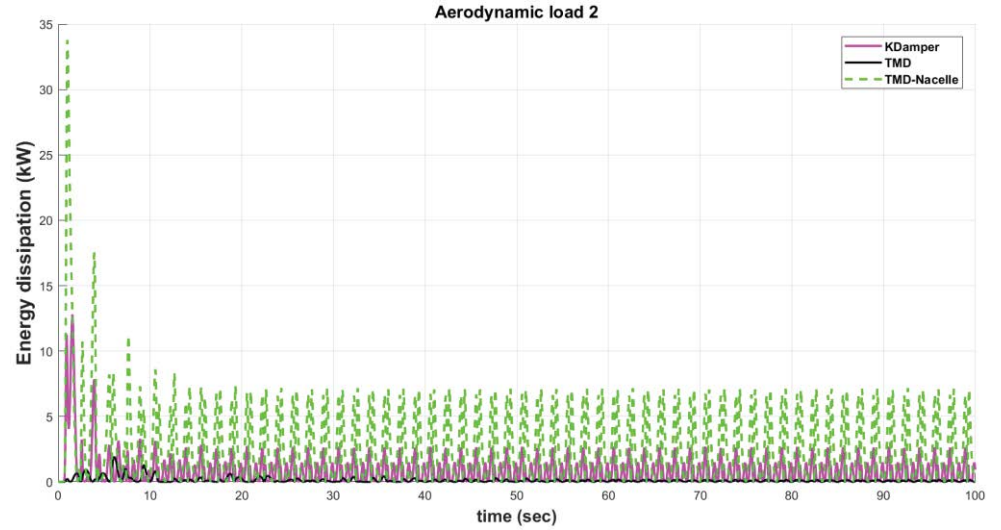

Fig. 9: Energy dissipation for Aerodynamic load 2

5 CONCLUSIONS

In this paper, three dynamic vibration absorber options are examined for improving the wind turbine's dynamic behavior, while also satisfying some certain constraints, the TMD, KDamper and Nacelle-isolation concepts. A wind turbine of 5MW supported by a steel tower of 120 m was analyzed under two different horizontal aerodynamic loads due to the wind. Based on the dynamic analysis and the results collected, the following conclusive observations can be made:

- Concerning the dynamic behavior of the wind turbine tower, the nacelle isolation concept yielded the best results along with the KDamper concept, with which the differences are minimal, followed by the TMD concept.
- Concerning the nacelle's velocity, all three concepts yielded the desirable results, reducing the maximum velocity for the aerodynamic load 1 by roughly 50%. For the aerodynamic load 2, the results can still be considered satisfactory as neither of the proposed concepts produced results close to the 1 *m/s* constraint that was set beforehand.
- The KDamper concept achieves better results than the TMD concepts and roughly the same as the nacelle-isolation concept with only 1/5 of the TMD's additional mass.
- The KDamper shows promising behavior in dissipating the energy of the aerodynamic loads and this energy can be gathered, further increasing the efficiency of the system.

According to the observations made above, the KDamper device can bring a realistic alternative to the existing vibration absorption design options in wind turbine towers, enhancing the dynamic performance both of the nacelle and the tower. The reliability and simplicity of the system are also benefits that render the device appropriate for various technological implementations and competitive against other vibration absorption designs.

REFERENCES

[1] M. Morais, M. Barcelos, S. Avila, M. Szhu, and de C. S. R., "Dynamic behavior analysis of Wind Turbine towers.," in *Congreso de Métodos Numéricos en Ingeniería*, 2009.

[2] S. Nigdeli and G. Bekdas, "Optimum tuned mass damper design in frequency domain for structures.," *KSCE J Civ Eng*, no. 21, pp. 912–922, 2016.

[3] S. Avila, M. Shzu, W. Pereira, L. Santos, M. Morais, and Z. Prado, "Numerical Modeling of the Dynamic Behavior of a Wind Turbine Tower.," *Art Adv Vibr Eng*, no. 4, 2016.

[4] G. Stewart and M. Lackner, "The impact of passive tuned mass dampers and wind-wave misalignment on offshore wind turbine loads.," *Eng Str*, no. 73, pp. 54–61, 2014.

[5] M. Lackner and M. Rotea, "Passive structural control of offshore wind turbines. Wind Energy," *Wind Energy*, no. 14, pp. 373–388, 2011.

[6] T. Soong and G. Dargush, *Passive Energy Dissipation Systems in Structural Engineering*. Wiley, 1997.

[7] F. Casciati and F. Giuliano, "Performance of a multi-tmd in the towers of suspension bridges," *J Vib Con*, no. 15, pp. 821–847, 2009.

[8] H. Frahm, "Device for Damping Vibrations of Bodies," 989958, 1909.

[9] J. Ormondroyd and J. Den Hartog, "The Theory of Dynamic Vibration Absorber," *Trans. ASME*, no. 50, pp. 9–22, 1928.

[10] J. Den Hartog, *Mechanical Vibrations*, 4th ed. McGraw Hill, 1956.

[11] N. Debnath, S. Deb, and A. Dutta, "Multi-modal vibration control of truss bridges with tuned mass dampers under general loading," *J Vib Con*, no. 22, pp. 4121–4140, 2015.

[12] A. Younespour and H. Ghaffarzadeh, "Structural active vibration control using active mass damper by block pulse functions," *J Vib Con*, no. 21, pp. 2787–2795, 2015.

[13] F. Ricciardelli, D. Pizzimenti, and M. Mattei, "Passive and active mass damper control of the response of tall buildings to wind gustiness," *Eng Str*, no. 25, pp. 1199–1209, 2003.

[14] S. Ankireddi and H. Yang, "Simple tmd control methodology for tall buildings subject to wind loads," *J Str Eng*, no. 122, pp. 83–91, 1996.
[15] S. Colwell and B. Basu, "Tuned liquid column dampers in offshore wind turbines for structural control," *Eng Str*, no. 31, pp. 358–368, 2009.
[16] F. Oliveira, A. Gomez, S. Avila, and J. Brito, "Design criteria for a pendulum absorber to control high building vibrations," *Int J IMSE*, no. 1, pp. 82–89, 2014.
[17] R. Skinner, W. Robinson, and G. McVerry, *An Introduction to Seismic Isolation*. New York: John Wiley & Sons, 1999.
[18] S. Deb, "Seismic base isolation – an overview," *Cur Sc*, no. 87, pp. 1426–1430, 2004.
[19] Govardhan, D. Paul, and Y. Singh, "Seismic Base Isolation An- overview," in *National Conference on Trends and Challenges in Structural Engineering and Construction Technique at CBRI*, 2008.
[20] J. Kelly, *Earthquake-Resistant Design with Rubber*, 2nd ed. London: Springer-Verlag, 1996.
[21] Govardhan, D. Paul, R. Jain, and S. Bagchi, "Design and Development of the base isolation system for Seismic protection of buildings," in *7th world congress on Joints, Bearings, and Seismic systems*, 2011.
[22] M. Kunde and R. Jangid, "Seismic behavior of isolated bridges: A-state-of-the-art review," *El J Str Eng*, no. 3, pp. 142–170, 2003.
[23] N. Grant, L. Fenves, and F. Auricchio, "Bridge isolation with high-damping rubber bearings – analytical modeling and system response," in *13th World Conference on Earthquake Engineering*, 2004.
[24] I. A. Antoniadis, S. Kanarachos, K. Gryllias, and I. E. Sapountzakis, "KDamping: A stiffness based vibration absorption concept," *J Vib Con*, no. 24, pp. 1–19, 2016.
[25] I. A. Antoniadis, K. A. Kapasakalis, and E. I. Sapountzakis, "Isolation or Damping? A Soil-dependent approach based on the KDamper concept.," in *ICONHIC*, 2019.
[26] E. I. Sapountzakis, K. A. Kapasakalis, and I. A. Antoniadis, "Negative Stiffness Elements in Seismic Isolation of Bridges.," in *ICONHIC*, 2019.
[27] K. A. Kapasakalis, C.-H. Alamir, I. A. Antoniadis, and E. I. Sapountzakis, "Frequency Base Design of the KDamper Concept for Seismic Isolation of Bridges.," in *ICOVP*, 2019.
[28] P. O. N. Bollano, K. A. Kapasakalis, E. I. Sapountzakis, and I. A. Antoniadis, "Design and Optimization of the KDamper Concept for Seismic Protection of Bridges," *Proc. 14th Int. Conf. Vib. Probl. (ICOVP 2019)*, vol. 1, 2019.
[29] K. A. Kapasakalis, I. A. Antoniadis, and E. I. Sapountzakis, "Implementation of the KDamper Concept for Seismic Protection of Bridges.," *ICOVP*, 2019.
[30] K. A. Kapasakalis, E. I. Sapountzakis, and I. A. Antoniadis, "Implementation of the KDamper concept to wind turbine towers," in *Compdyn*, 2017.
[31] K. A. Kapasakalis, E. I. Sapountzakis, and I. A. Antoniadis, "Optimal Design of the KDamper Concept for Structures on Compliant Supports.," in *ECEE*, 2018.
[32] K. A. Kapasakalis, E. I. Sapountzakis, and I. A. Antoniadis, "KDamper Concept in Seismic Isolation of Multi Storey Building Structures," in *GRACM*, 2018.
[33] K. A. Kapasakalis, E. I. Sapountzakis, and I. A. Antoniadis, "Kdamper concept in seismic isolation of building structures with soil structure interaction.," in *Conf. Comput. Struct. Technol*, 2018.
[34] K. A. Kapasakalis, E. I. Sapountzakis, and I. A. Antoniadis, "Control of Multi Storey Building Structures with a New Passive Vibration Control System Combining Base Isolation with KDamper.," in *Compdyn*, 2019.
[35] K. A. Kapasakalis, E. I. Sapountzakis, and I. A. Antoniadis, "Implementation of the

KDamper Concept for Base Isolation to a Typical Concrete Building Structure.," in *Int. Congr. Mech*, 2019.

[36] K. A. Kapasakalis, I. A. Antoniadis, and E. I. Sapountzakis, "KDamper Concept for Base Isolation and Damping of High-Rise Building Structures.," in *ICOVP*, 2019.

[37] I. A. Antoniadis, K. A. Kapasakalis, and E. I. Sapountzakis, "Advanced Negative Stiffness Absorbers for the Seismic Protection of Structures.," in *Int. Conf. Key Enabling Technol.*, 2019.

[38] K. A. Kapasakalis, I. A. Antoniadis, and E. I. Sapountzakis, "Novel Vibration Absorption Systems with Negative Stiffness Elements for the Seismic Protection of Structures.," in *Natl. Conf. Earthq. Eng. Eng. Seismol*, 2019.

[39] K. A. Kapasakalis, I. A. Antoniadis, and E. I. Sapountzakis, "Performance Assessment of the KDamper as a Seismic Absorption Base.," in *Struct. Control Heal Monit.*, 2019.

[40] K. A. Kapasakalis, I. A. Antoniadis, and E. I. Sapountzakis, "Implementation of the KDamper as a Stiff Seismic Absorption Base: A Preliminary Assessment," *Vib. Acoust. Res. J.*, vol. 1, no. 1, pp. 1–26, 2019.

[41] S. Bhattacharya and S. Adhikari, "Experimental Validation of Soil-Structure Interaction of Offshore Wind Turbines," *Soil Dyn Ear Eng*, no. 31, pp. 805–816, 2011.

[42] A. Quiligan, A. O'Connor, and V. Pakrashi, "Fragility Analysis of Steel and Concrete Wind Turbine Towers," *Eng Str*, no. 36, pp. 270–282, 2012.

[43] M. Hansen, *Aerodynamics of Wind Turbines*, 2nd ed. Earthscan, 2008.

[44] CEN/TC250, "Eurocode 1: Actions on structures-General actions-Part 1-4: Wind actions." 2004.

[45] K. Koulatsou, F. Petrini, S. Vernardos, and C. Gantes, "Artificial Time Histories of Wind Actions for Structural Analysis of Wind Turbines," in *BCCCE*, 2013.

[46] M. Di Paola, "Digital Simulation of Wind Field Velocity," *J Wind Eng Ind Aerodyn*, pp. 74–76, 91–109, 1998.

[47] DNV/Risø, *Guidelines for Design of Wind Turbines*. Denmark, 2002.

[48] J. Jonkman, "Dynamics Modeling and Loads Analysis of an Offshore Floating Wind Turbine," 2007.

[49] Y. Shkara, M. Cardaun, R. Schelenz, and G. Jacobs, "Aeroelastic response of a multi-megawatt upwind HAWT based on fluid-structure interaction simulation," *Wind Energy Sci.*, pp. 10–12, 2019.